Electronic Supplementary Material (ESI) for Physical Chemistry Chemical Physics.

Supporting Information

Interstitial or Interstitialcy: Effect of the Cation Size on the Migration Mechanism in NaSICON Materials

Judith Schütt,[a,b] Johanna Schillings,[a] Steffen Neitzel-Grieshammer[c]

[a.] Institute of Physical Chemistry, RWTH Aachen University, 52056 Aachen, Germany.

[b.] Helmholtz-Institut Münster (IEK-12), Forschungszentrum Jülich GmbH, 48149 Münster, Germany.

[c.] Department of Chemical Engineering, FH Münster University of Applied Sciences, 48565 Steinfurt, Germany.

1. Computational Details

The Shannon radius[1] of the cations in $Na_{1+x}M_2Si_xP_{3-x}O_{12}$ and the valence electrons for all elements considered in the calculations of $Na_{1+x}M_2Si_xP_{3-x}O_{12}$ are listed in Table S1.

Table S1. Ionic cation radius according to Shannon[1] and valence electrons for all elements considered in the calculations of $Na_{1+x}M_2Si_xP_{3-x}O_{12}$.

Element	$r_{Shannon}$ (Å)	Valence electrons
O^{2-}		$2s^2 2p^4$
Na^{+}		$2p^6 3s^1$
P^{5+}	0.17	$3s^2 3p^3$
Si^{4+}	0.40	$3s^2 3p^2$
Ge^{4+}	0.53	$3d^{10} 4s^2 4p^2$
Cr^{4+}	0.55	$3p^6 3d^5 4s^1$
V^{4+}	0.58	$3s^2 3p^6 3d^3 4s^2$
Ti^{4+}	0.61	$3s^2 3p^6 3d^2 4s^2$
Mo^{4+}	0.65	$4p^6 4d^5 5s^1$
W^{4+}	0.66	$5p^6 5d^4 6s^2$
Nb^{4+}	0.68	$4s^2 4p^6 4d^4 5s^1$
Sn^{4+}	0.69	$4d^{10} 5s^2 5p^2$
Hf^{4+}	0.71	$5p^6 5d^2 6s^2$
Zr^{4+}	0.72	$4s^2 4p^6 4d^2 5s^2$
Pb^{4+}	0.78	$5d^{10} 6s^2 6p^2$
Ce^{4+}	0.87	$4f^2 5s^2 5p^6 6s^2$

2. Na^+ Site Energy

2.1 Na^+ Site Energy in Na*M*P

We propose that the stability of the Na^+ ion configurations is governed on the one hand by electrosteric repulsion of the Na2 and Na3, and on the other hand by the stabilization of V_{Na1} by adjacent Na2 and Na3 ions, which compensate for the missing charge of the unoccupied Na1 site.

Two limiting cases elucidate this interplay: When the distances $d_{Na\text{-}V_{Na1}}$ between Na2 or Na3 ions and V_{Na1} are large, only the energetically most favourable configuration (0a) exists, as the electrosteric repulsion effects are insufficient to prevent one of the Na2 or Na3 ions from occupying the energetically preferred Na1 site. Therefore, configuration (0b) is not observed for compounds with medium to large M^{4+} ions when the Na2 ions are aligned at 90° and 180°.

Conversely, strong electrosteric repulsion prevents the formation of configurations with very small distances $d_{Na\text{-}Na}$ of Na2-Na2 or Na3-Na3 pairs. Hence, configuration (0c) is not observed when two Na3 ions are aligned at 80°.

To validate this assumption, Figure S1 examines the distances $d_{Na\text{-}Na}$ and $d_{Na\text{-}V_{Na1}}$ as a function of the size of the M^{4+} cations in Na*M*P. Figure S2 and Figure S4 depict the corresponding E_{conf} as a function of $d_{Na\text{-}Na}$, while Figure S3 and Figure S5 illustrate E_{conf} as a function of $d_{Na\text{-}V_{Na1}}$. Figure S6 combines the results by depicting E_{conf} as a function of both the the distance $d_{Na\text{-}Na}$ and $d_{Na\text{-}V_{Na1}}$. From this, the following conclusions can be drawn:

(i) $d_{Na\text{-}V_{Na1}}$ is smaller for Na3 than for Na2 explaining the energetic preference of configuration (0c) over configuration (0b) by stronger stabilization of V_{Na1}, since smaller distances between Na^+ and V_{Na1} possibly counterbalance more strongly the missing charge of the unoccupied Na1 site. Smaller $d_{Na\text{-}Na}$ between Na3 ions compared to Na2 ions, leading to a more pronounced electrosteric repulsion effects, seems to have a minor impact here.

(ii) As the angle between the Na2 or Na3 ions increases, $d_{Na\text{-}V_{Na1}}$ contracts while $d_{Na\text{-}Na}$ expands. Both effects contribute to the reduction of E_{conf}, which can be attributed to the decreasing electrosteric repulsion effects and the establishment of a more balanced local charge, as described above.

(iii) $d_{Na\text{-}Na}$ increases with the size of the M^{4+} cations, leading to the decrease of E_{conf} due to weaker repulsive Na^+-Na^+ interactions. This effect is contradicted by the simultaneous increase of $d_{Na\text{-}V_{Na1}}$. Nevertheless, the increase in both $d_{Na\text{-}Na}$ and $d_{Na\text{-}V_{Na1}}$ with the M^{4+} cation size is small, suggesting only minor impact on the local charge balance but a more pronounced influence on the electrosteric repulsion effects.

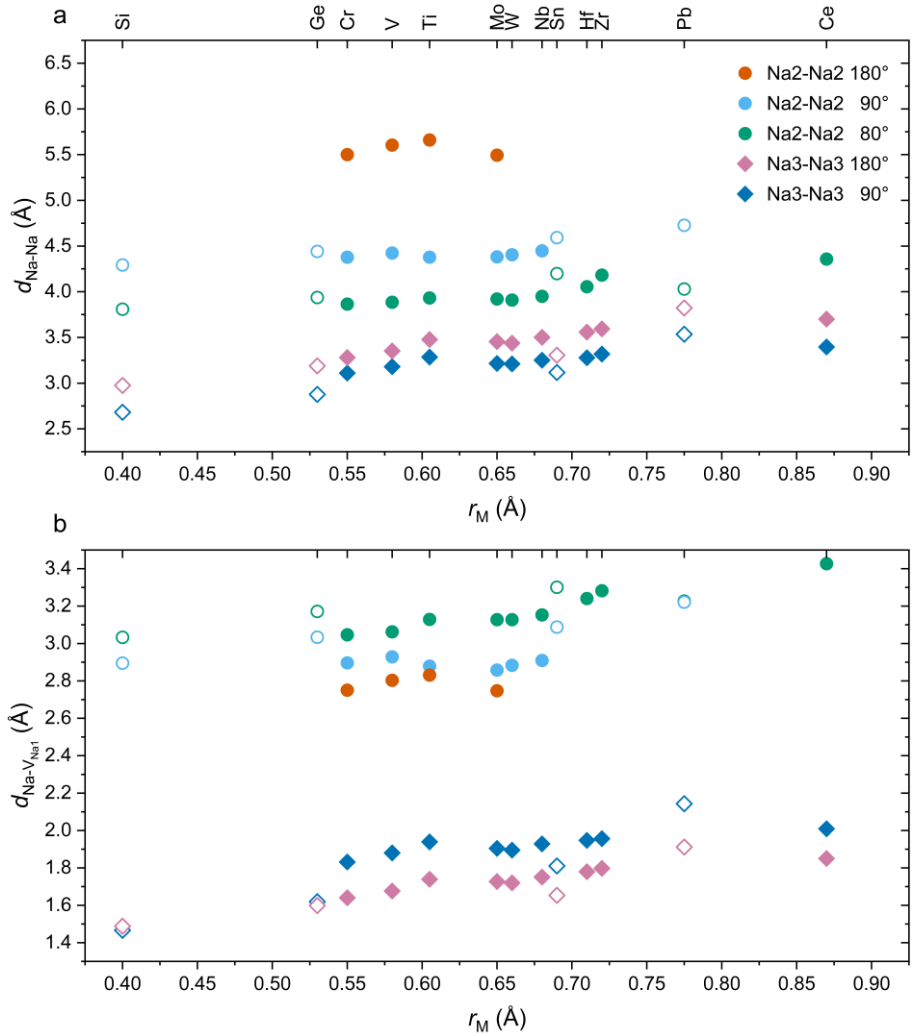

Figure S1. (a) Distance $d_{Na\text{-}Na}$ between the Na2 or Na3 ions, and (b) distance $d_{Na\text{-}V_{Na1}}$ between the Na2 or Na3 ions and Na1 vacancy V_{Na1} for configurations (0b) and (0c) in Na*M*P. In configuration (0b), the Na2 ions are arranged at 80° (green), 90° (light blue), 180 ° (red), and in configuration (0c), the Na3 ions are arranged at 90° (dark blue), 180° (purple). The distance is shown as a function of the Shannon radius r_M[1] of the M^{4+} cations (closed symbols: M^{4+} transition metals, open symbols: M^{4+} main group elements).

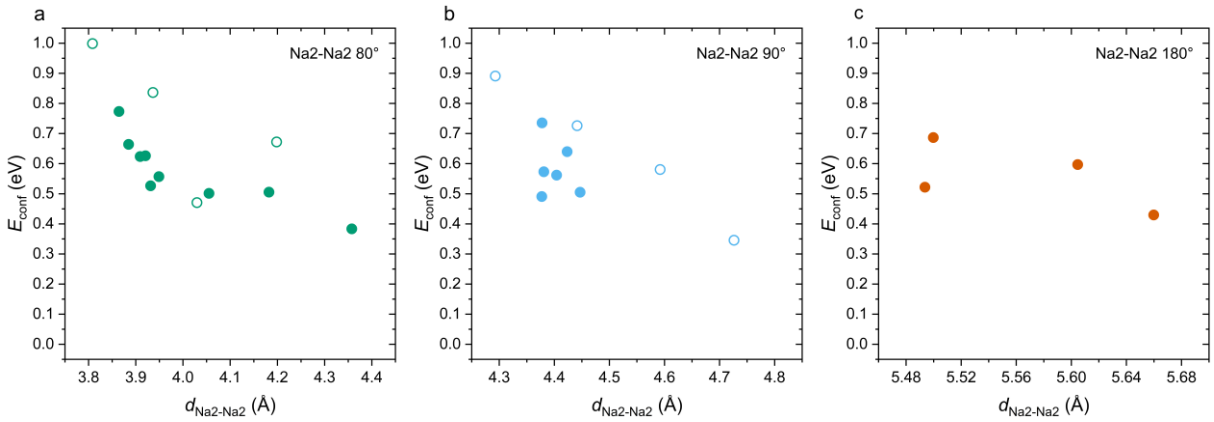

Figure S2. Energy E_{conf} of the configuration (0b) in Na*M*P with different M^{4+} cations (closed symbols: M^{4+} transition metals, open symbols: M^{4+} main group elements). E_{conf} is shown as a function of the distance $d_{Na2\text{-}Na2}$ between the Na2 ions arranged at (a) 80°, (b) 90°, and (c) 180°.

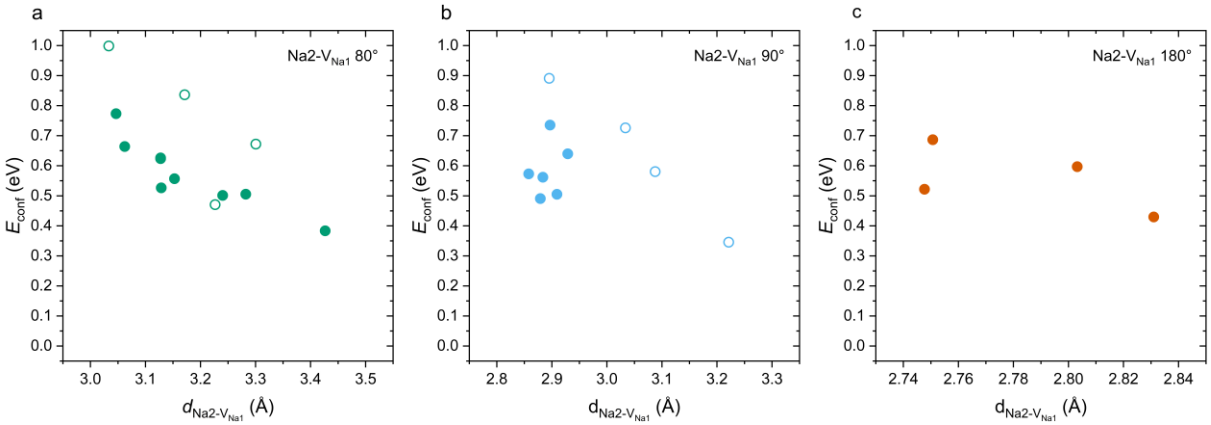

Figure S3. Energy E_{conf} of the configuration (0b) in NaMP with different M^{4+} cations (closed symbols: M^{4+} transition metals, open symbols: M^{4+} main group elements). E_{conf} is shown as a function of the distance $d_{Na2\text{-}V_{Na1}}$ between the Na2 ions and Na1 vacancy V_{Na1} for (a) 80°, (b) 90°, and (c) 180°.

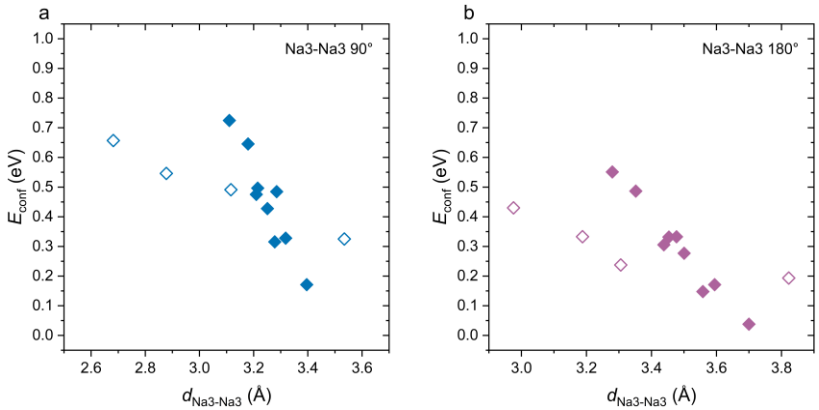

Figure S4. Energy E_{conf} of the configuration (0c) in NaMP with different M^{4+} cations (closed symbols: M^{4+} transition metals, open symbols: M^{4+} main group elements). E_{conf} is shown as a function of the distance $d_{Na3\text{-}Na3}$ between the Na3 ions arranged at (a) 90°, and (b) 180°.

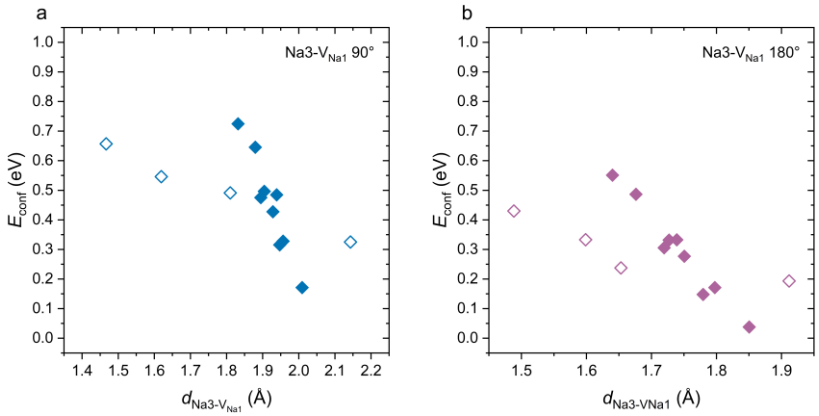

Figure S5. Energy E_{conf} of the configuration (0c) in NaMP with different M^{4+} cations (closed symbols: M^{4+} transition metals, open symbols: M^{4+} main group elements). E_{conf} is shown as a function of the distance $d_{Na3\text{-}V_{Na1}}$ between the Na3 ions and Na1 vacancy V_{Na1} for (a) 90°, and (b) 180°.

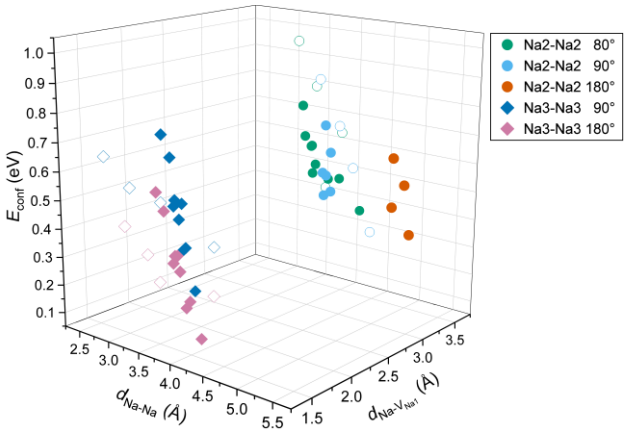

Figure S6. Energy E_{conf} of configuration (0b), in which two Na2 ions are arranged at 80° (green), 90° (light blue), 180° (red), and configuration (0c), in which two Na3 ions are arranged at 90° (dark blue), 180° (purple), in Na*M*P with different M^{4+} cations (closed symbols: M^{4+} transition metals, open symbols: M^{4+} main group elements). E_{conf} is shown as a function of the distance d_{Na-Na} between Na2 or Na3 ions as well as the distance $d_{Na-V_{Na1}}$ between the Na2 or Na3 ions and Na1 vacancy V_{Na1}.

It is worth noting that the increase of the size of M^{4+} cations in NaMP results in the expansion of its structural framework. Consequently, the distances between Na^+ and the scaffold ions increase, which may further affect the incorporation of the Na^+ ions within the framework. Figure S7 depicts the increase in the Na^+-P^{5+}-, Na^+-M^{4+}-, and Na^+-O^{2-}-distances with the size of the M^{4+} cations.

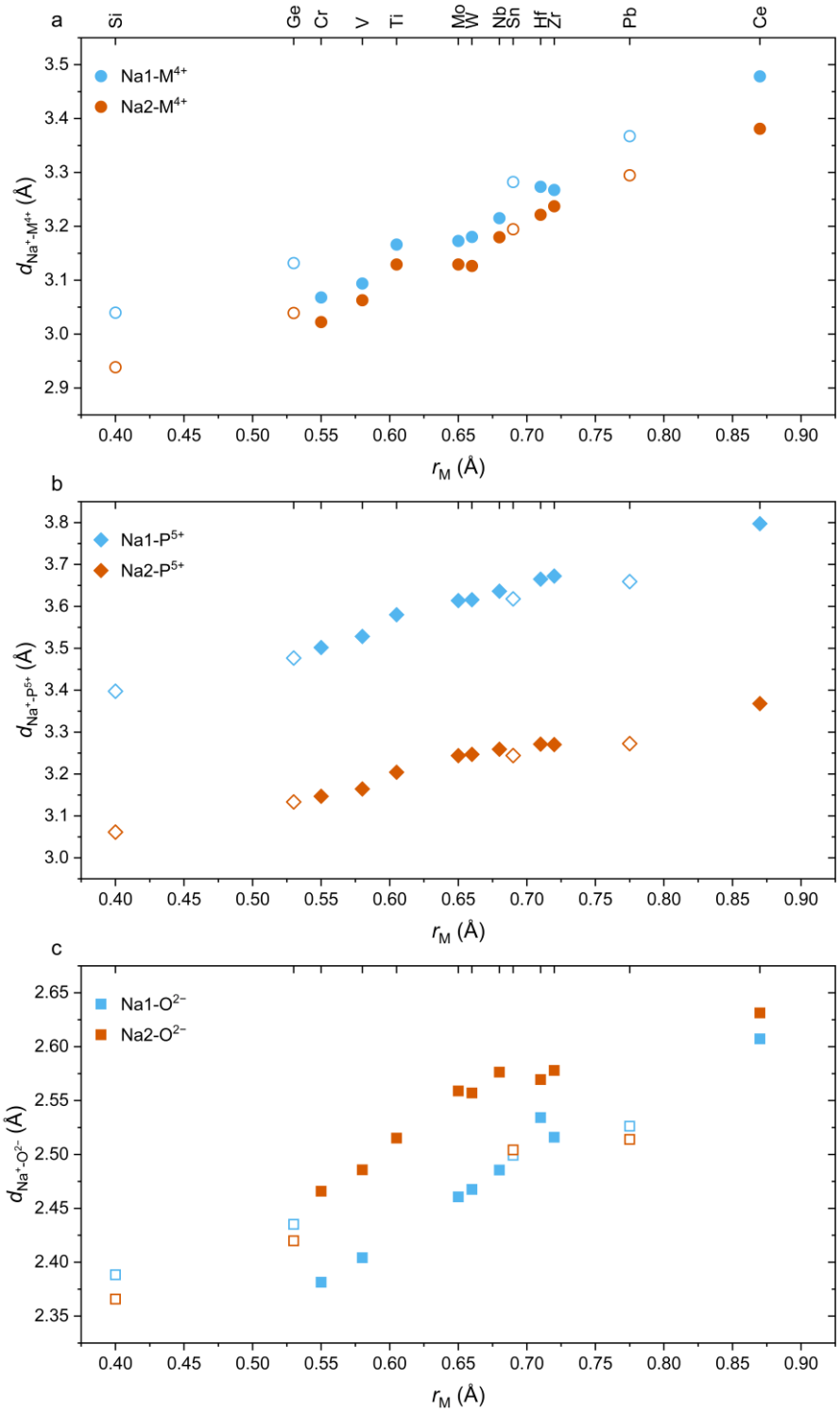

Figure S7. Distance d between the Na^+ ions and the framework ions as a function of the Shannon radius r_M[1] of the M^{4+} cations (closed symbols: M^{4+} transition metals, open symbols: M^{4+} main group elements) in NaMP. Shown are the distances between

(a) Na-M^{4+}, (b) Na-P^{5+}, (c) Na-O^{2-}, with blue symbols denoting the distances of the Na1 ions and red symbols representing the distances of the Na2 ions.

2.2 Na^+ Site Energy in Na*M*Si

The impact of Na^+-Na^+ Coulombic repulsion and steric hindrance on the configuration energy E_{conf} in Na*M*Si is investigated. Therefore, Figure S8(a) shows $d_{Na2\text{-}Na2}$ of configuration (3b), while Figure S9 depicts $d_{Na3\text{-}Na3}$ and $d_{Na3\text{-}V_{Na1}}$ of configuration (3c) as a function of the size of the M^{4+} cations. In addition, E_{conf} of configuration (3b) is depicted as a function of $d_{Na2\text{-}Na2}$ in Figure S8(b), while E_{conf} of configuration (3c) is shown as a function of $d_{Na3\text{-}Na3}$ and $d_{Na3\text{-}V_{Na1}}$ in Figure S10 and Figure S11, respectively. No clear trend for the dependence of the E_{conf} of configuration (3b) on the Na2-Na2 distance and of configuration (3c) on the Na3-Na3 and Na3-V_{Na1} distance can be established. However, all energy values are rather small.

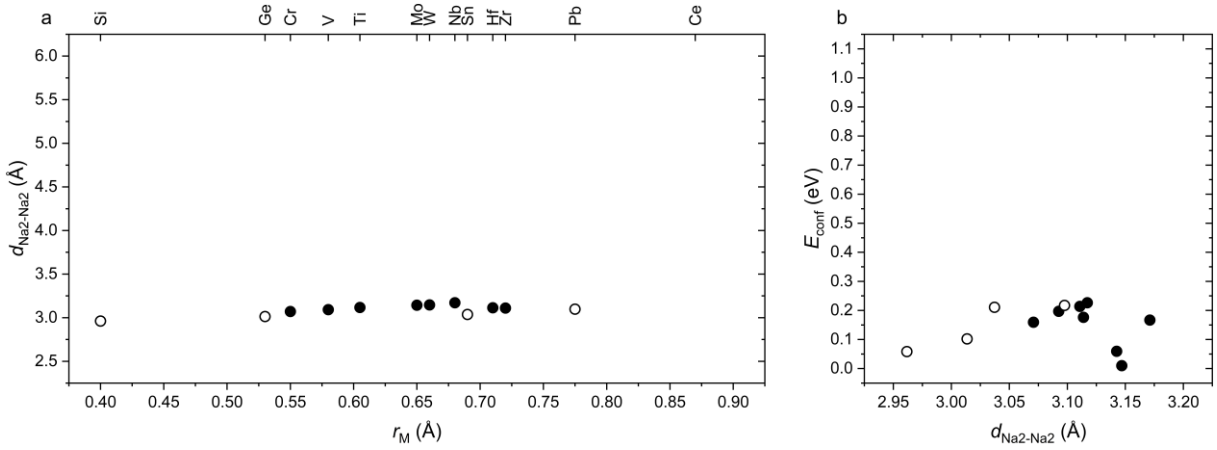

Figure S8. (a) Distance $d_{Na2\text{-}Na2}$ between the Na2 ions as a function of the Shannon radius r_M[1] of the M^{4+} cations, and (b) energy E_{conf} of the configuration (3b) as a function of $d_{Na2\text{-}Na2}$ in Na*M*Si with different M^{4+} cations (filled symbols: M^{4+} transition metals, empty symbols: M^{4+} main group elements).

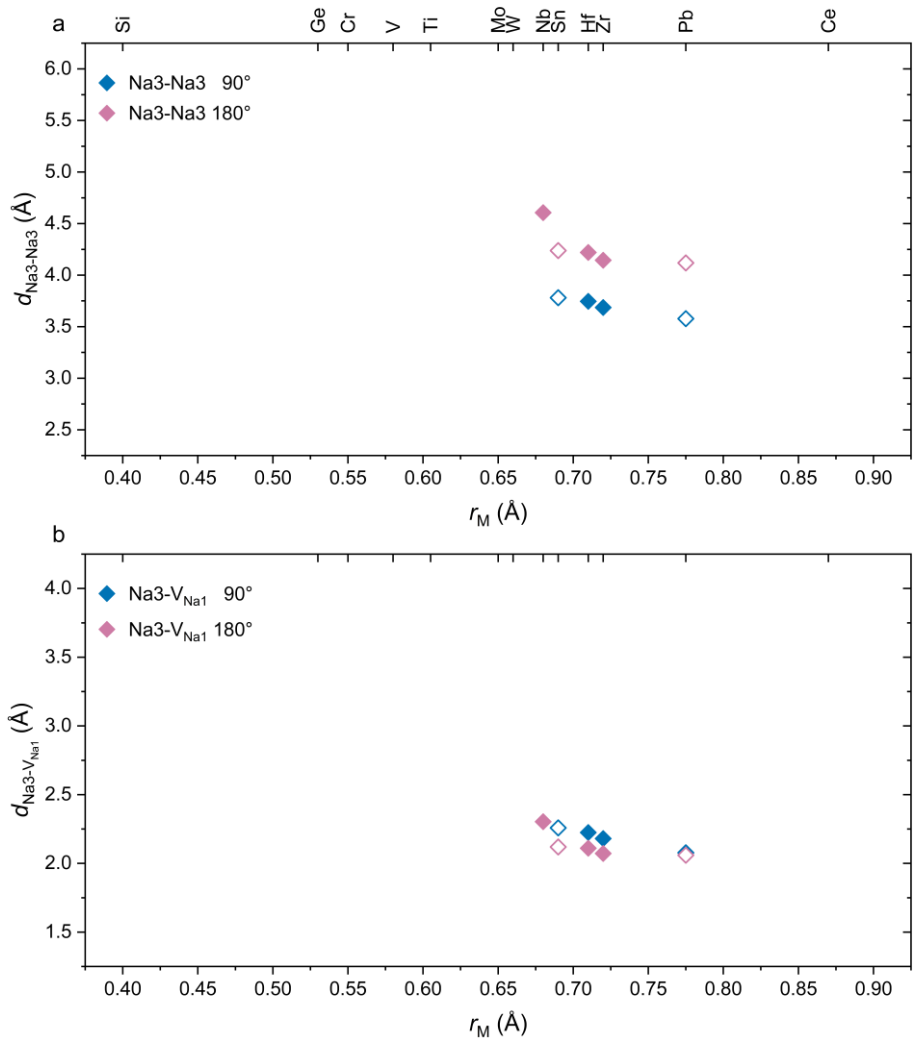

Figure S9. (a) Distance $d_{Na3\text{-}Na3}$ between the Na3 ions, and (b) distance $d_{Na3\text{-}V_{Na1}}$ between the Na3 ions and Na1 vacancy V_{Na1} for configuration (3c) in Na*M*Si. The Na3 ions are arranged at 90° (dark blue) and 180° (purple). The distance is shown as a function of the Shannon radius r_M[1] of the M^{4+} cations (closed symbols: M^{4+} transition metals, open symbols: M^{4+} main group elements).

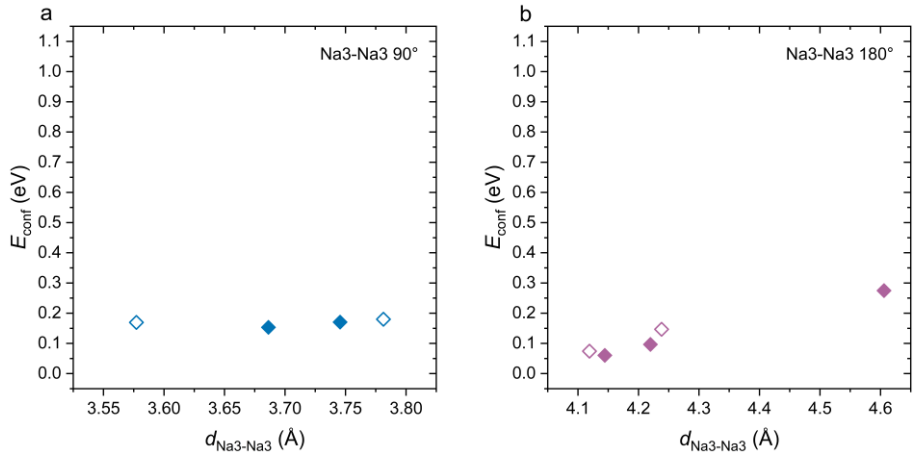

Figure S10. Energy E_{conf} of the configuration (3c) in Na*M*Si with different M^{4+} cations (filled symbols: M^{4+} transition metals, empty symbols: M^{4+} main group elements). E_{conf} is shown as a function of the distance $d_{Na3\text{-}Na3}$ between Na3 ions arranged at (a) 90° and (b) 180°.

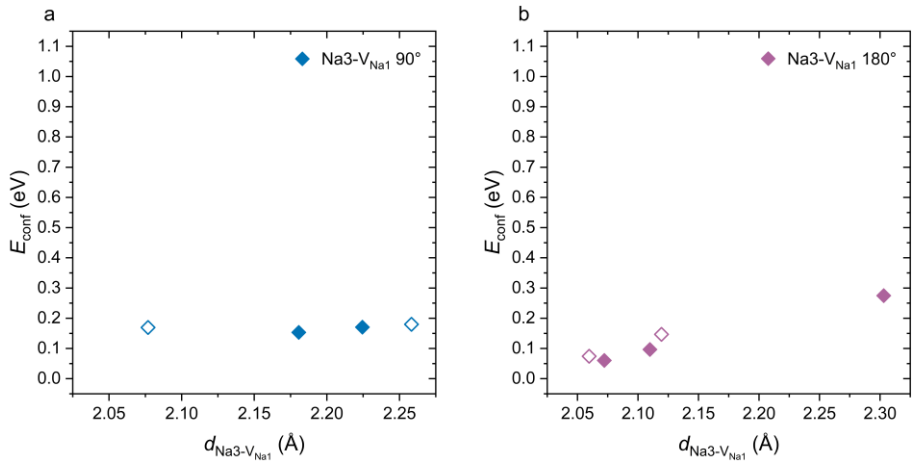

Figure S11. Energy E_{conf} of the configuration (3c) in Na*M*Si with different M^{4+} cations (closed symbols: M^{4+} transition metals, open symbols: M^{4+} main group elements). E_{conf} is shown as a function of the distance $d_{Na3\text{-}V_{Na1}}$ between the Na3 ions and the Na1 vacancy V_{Na1} arranged at (a) 90°, and (b) 180°.

3. Na^+ Ion Migration

3.1 Migration Mechanism

3.1.1 Interstital-like Mechanism

In the interstitial-like mechanism, shown in Figure S11, one Na1 ion jumps to an adjacent, unoccupied Na2 sites, resulting in a metastable transient state with one vacant Na1 site and two occupied Na2 sites adjacent to the Na1 vacancy. Subsequently, one Na2 ion jumps onto the Na1 vacancy. The bottlenecks of this migration, denoted as A and A', are formed by the PO_4/SiO_4- and MO_6-polyhedra edges.

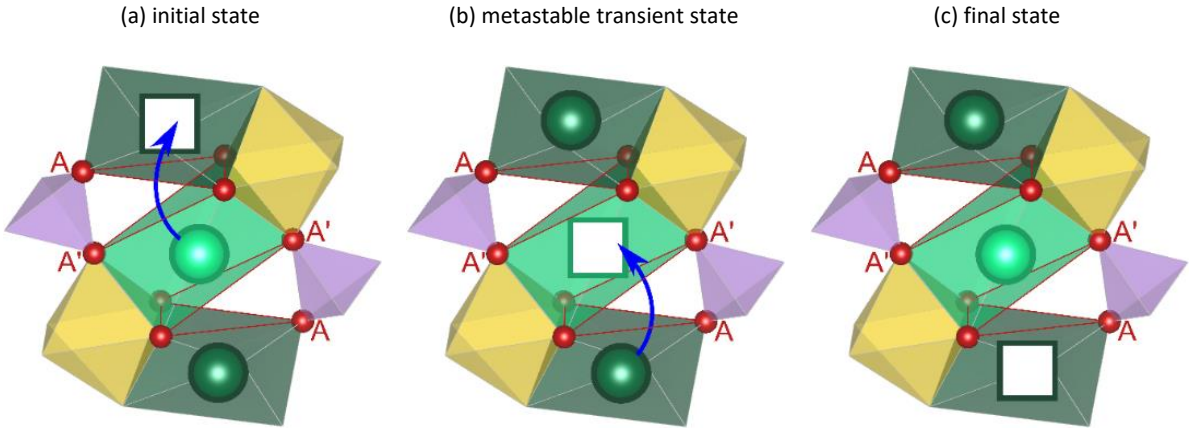

Figure S12. (a) Initial, (b) metastable transition, and (c) final state of the interstitial-like mechanism, shown with blue arrows. (a) The Na1 ion jumps onto an adjacent vacant Na2 site; (b) The metastable transition state with one vacant Na1 site V_{Na1} and two occupied Na2 sites is formed. Subsequently, the Na2 ion jumps onto V_{Na1}; (c) In the final state, the Na1 and one Na2 sites are occupied. The bottlenecks A and A' of the migration pathway formed by PO_4/SiO_4- and MO_6-polyhedra edges are depicted as red triangles. Key: Na^+ vacancy (empty box), Na1 (light green), Na2 (dark green), MO_6 (yellow), PO_4/SiO_4 (purple), O (red).

The true transition state is energetically and structurally close to the metastable transient state, as shown in Figure S13, which depicts the energy profile for the migration of the Na^+ ions by the interstitial-like mechanism in the direction of 180° within Na*M*P for *M* = V4+ and the corresponding alignment of the migrating Na^+ ions in the initial, transition, metastable transient and final state.

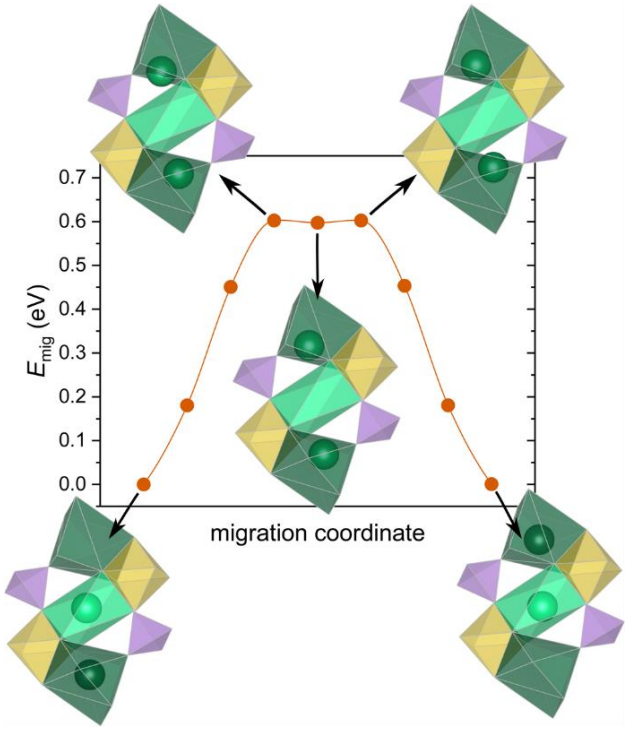

Figure S13. Energy profile for the Na^+ ion migration by the interstitial-like mechanism in 180° direction in Na*M*P for $M = V^{4+}$. The orientation of the migrating Na^+ ions in the initial, transition, metastable transient and final state is shown.

3.1.2 Interstitalcy-like Mechanism

The interstitialcy-like mechanism involves the simultaneous jump of Na1 and Na2 ions to their neighboring Na^+ sites, as illustrated in Figure S14. Na2 ions move towards occupied Na1 sites and Coulomb repulsion forces the Na1 ions onto adjacent unoccupied Na2 sites. Along the migration path, metastable transient split-pair positions are observed, wherein two Na^+ ions occupy Na3 site. The bottlenecks of this migration, denoted as A, A', B', and B, are formed by the PO_4/SiO_4- and MO_6-polyhedra edges.

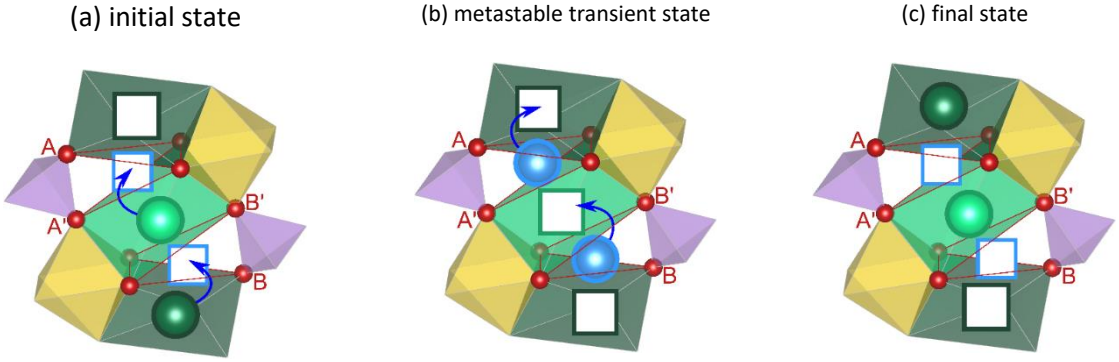

Figure S14. (a) Initial, (b) metastable transient, and (c) final state of interstitialcy-like mechanism, shown with blue arrows. (a), (c) One Na2 ion moves towards the Na1 site pushing it onto an adjacent unoccupied Na2 site; (b) The metastable transient split-pair position is formed, wherein two Na^+ ions occupy the Na3 sites. The bottlenecks A, A', B', and B of the migration pathway formed by PO_4/SiO_4- and MO_6-polyhedra edges are depicted as red triangles. Key: Na^+ vacancy (empty box), Na1 (light green), Na2 (dark green), MO_6 (yellow), PO_4/SiO_4 (purple), O (red).

3.2 Energy Profiles

3.2.1 Energy Profiles of the Interstital-like Mechanism

The calculated energy profiles of the interstitial-like mechanism for Na*M*P and Na*M*Si are shown in the following. It is worth noting that there is no directionality of the interstitial-like migration in Na*M*Si.

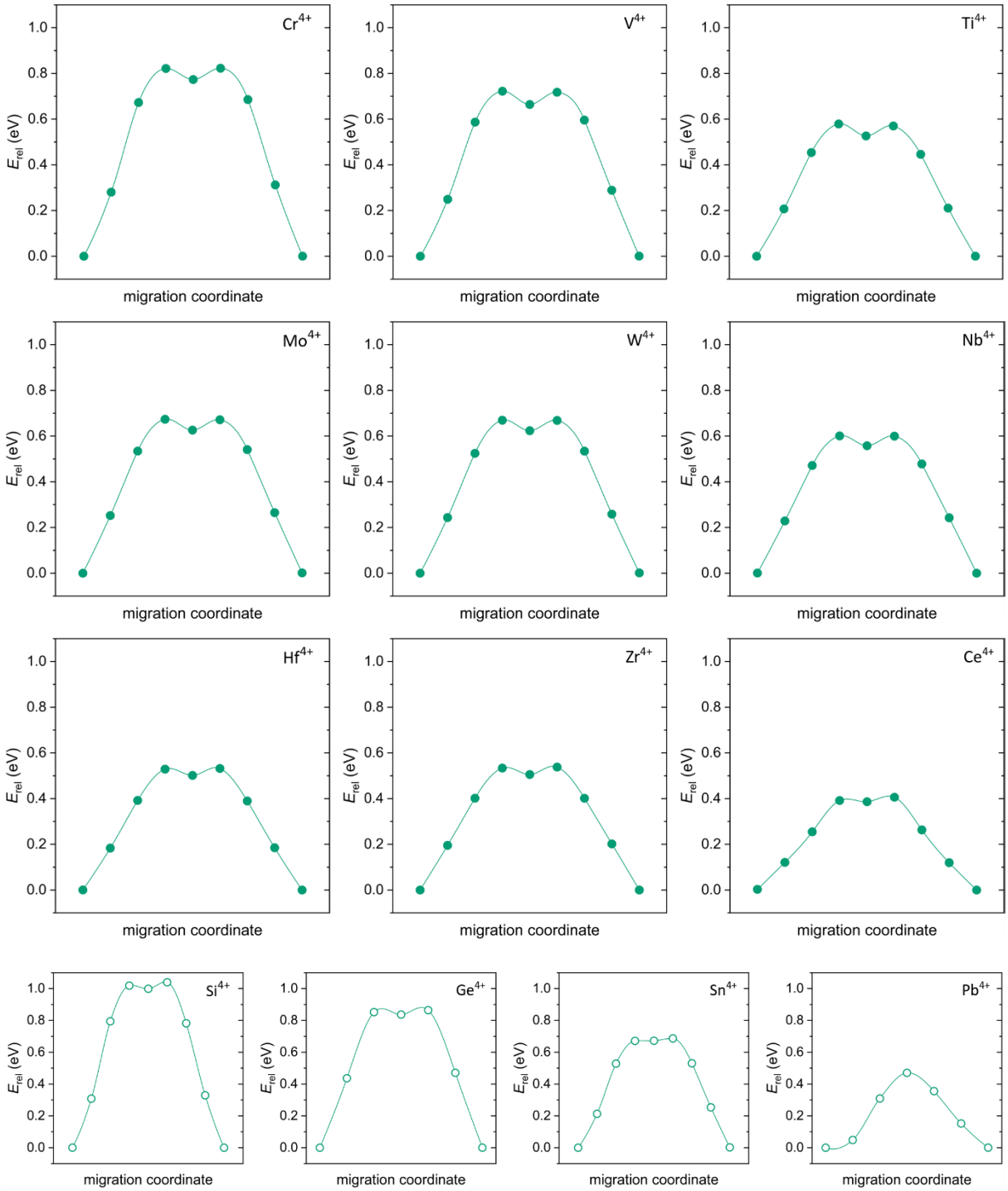

Figure S15. Energy profiles of interstitial-like migration in 80° in Na*M*P containing different M^{4+} cations.

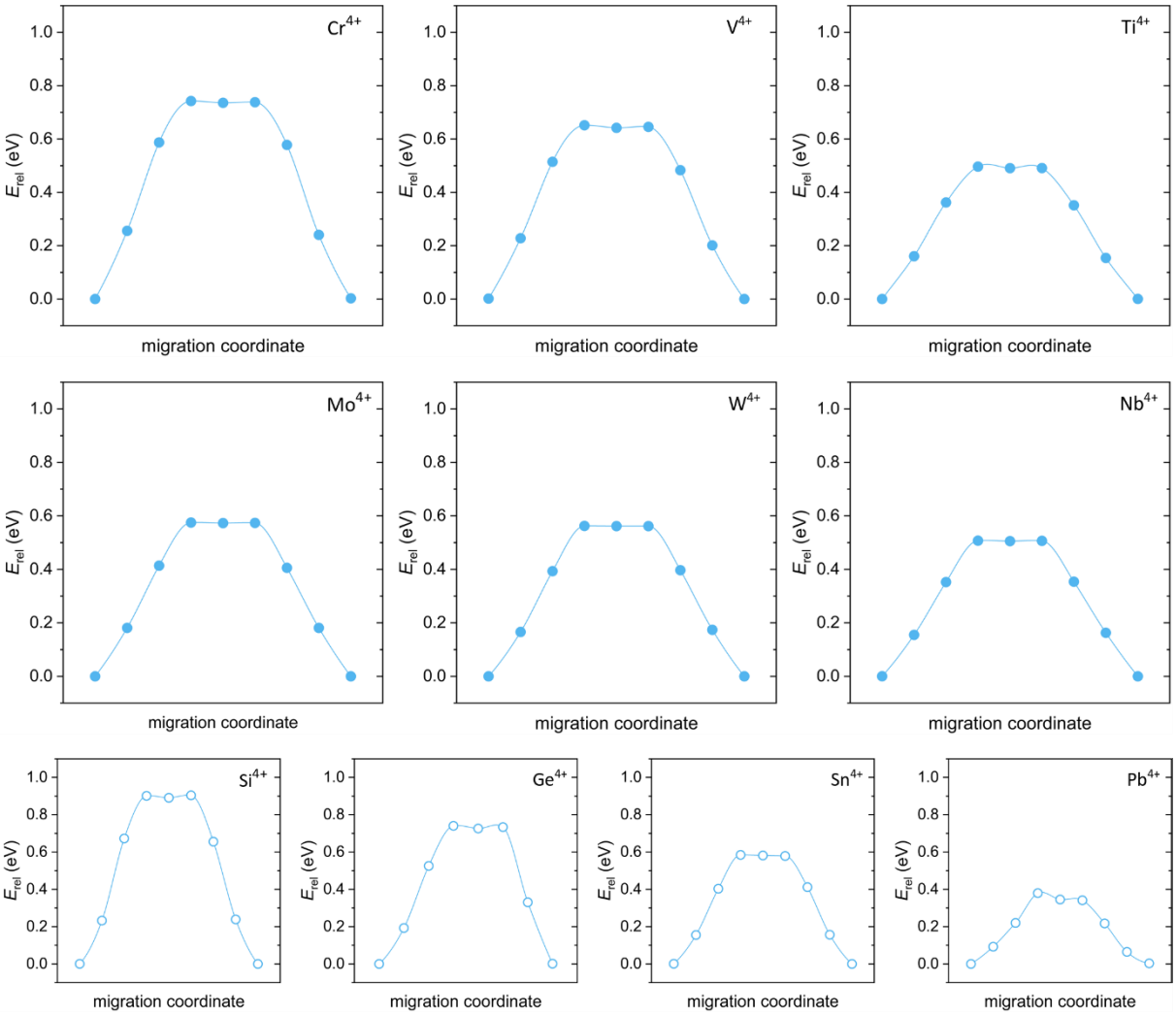

Figure S16. Energy profiles of interstitial-like migration in 90° in Na*M*P containing different M^{4+} cations.

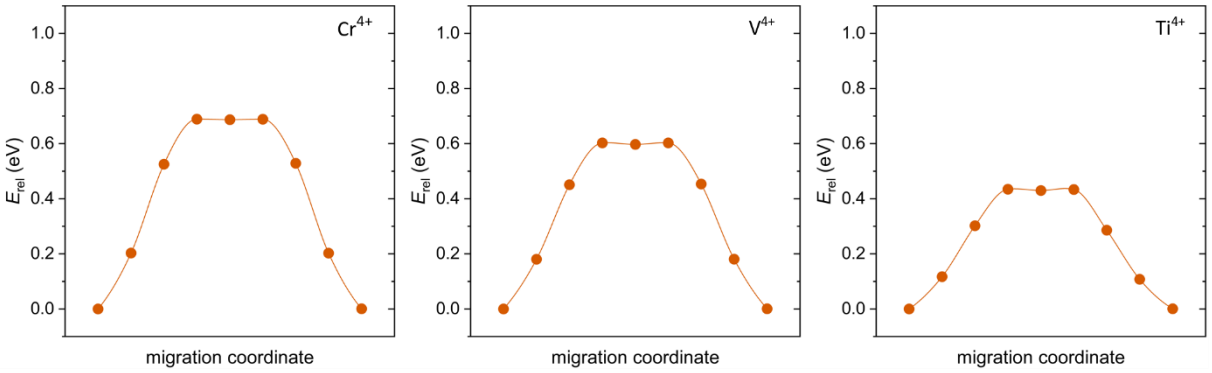

Figure S17. Energy profiles of interstitial-like migration in 180° in Na*M*P containing different M^{4+} cations.

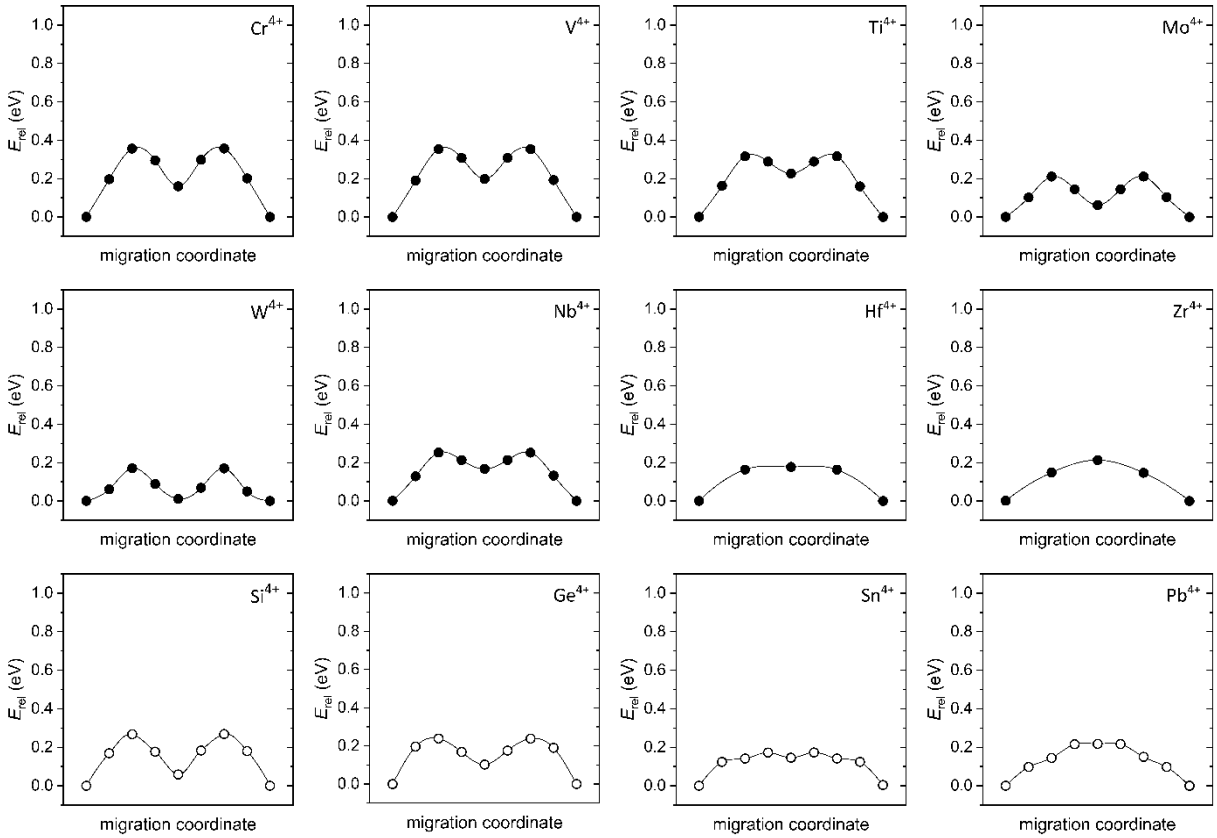

Figure S18. Energy profiles of interstitial-like migration in Na*M*Si containing different M^{4+} cations.

3.2.2 Energy Profiles of the Interstitialcy-like Mechanism

The calculated energy profiles of the interstitialcy-like mechanism for Na*M*P and Na*M*Si are shown in the following.

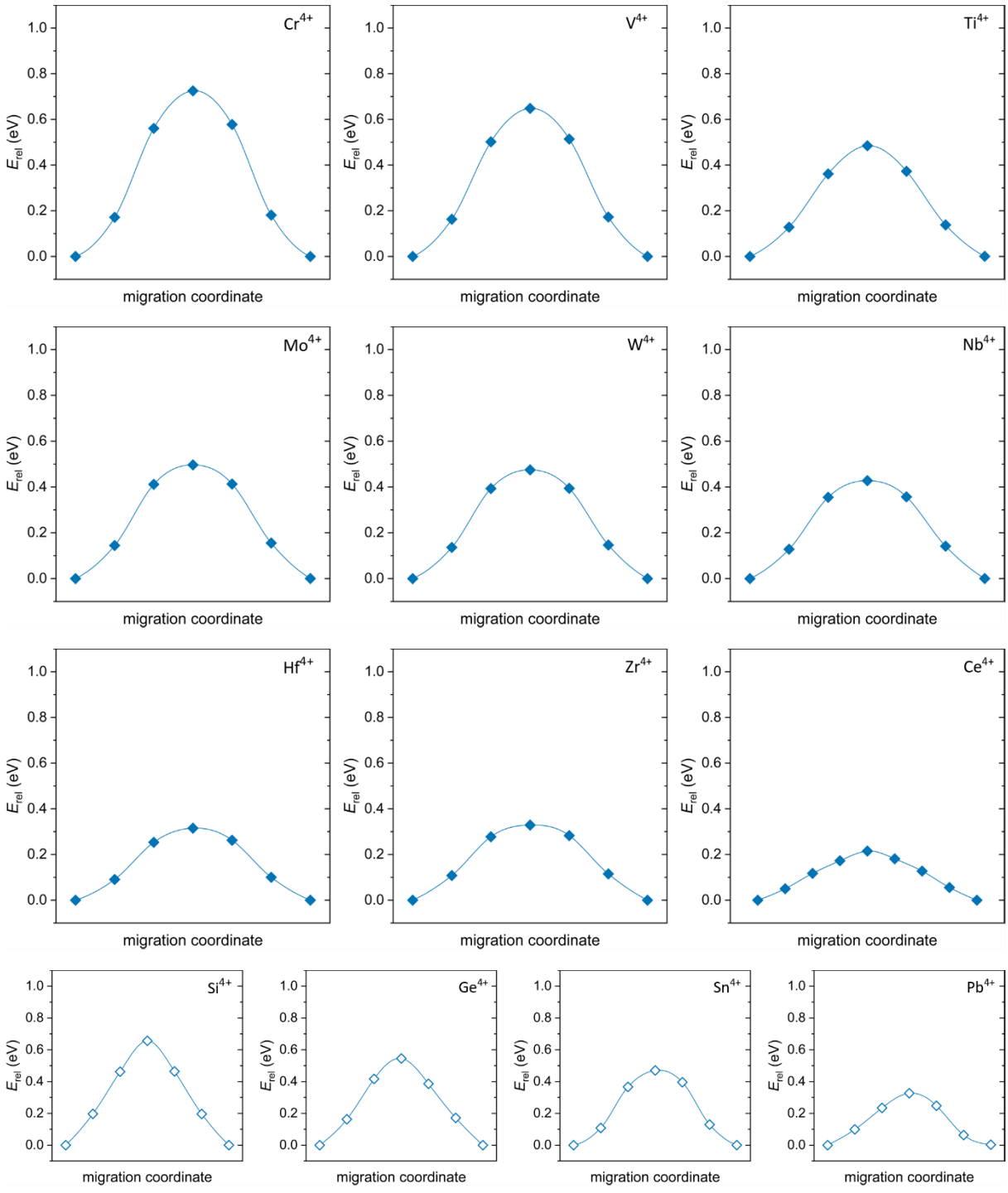

Figure S19. Energy profiles of interstitialcy-like migration in 90° in Na*M*P containing different M^{4+} cations.

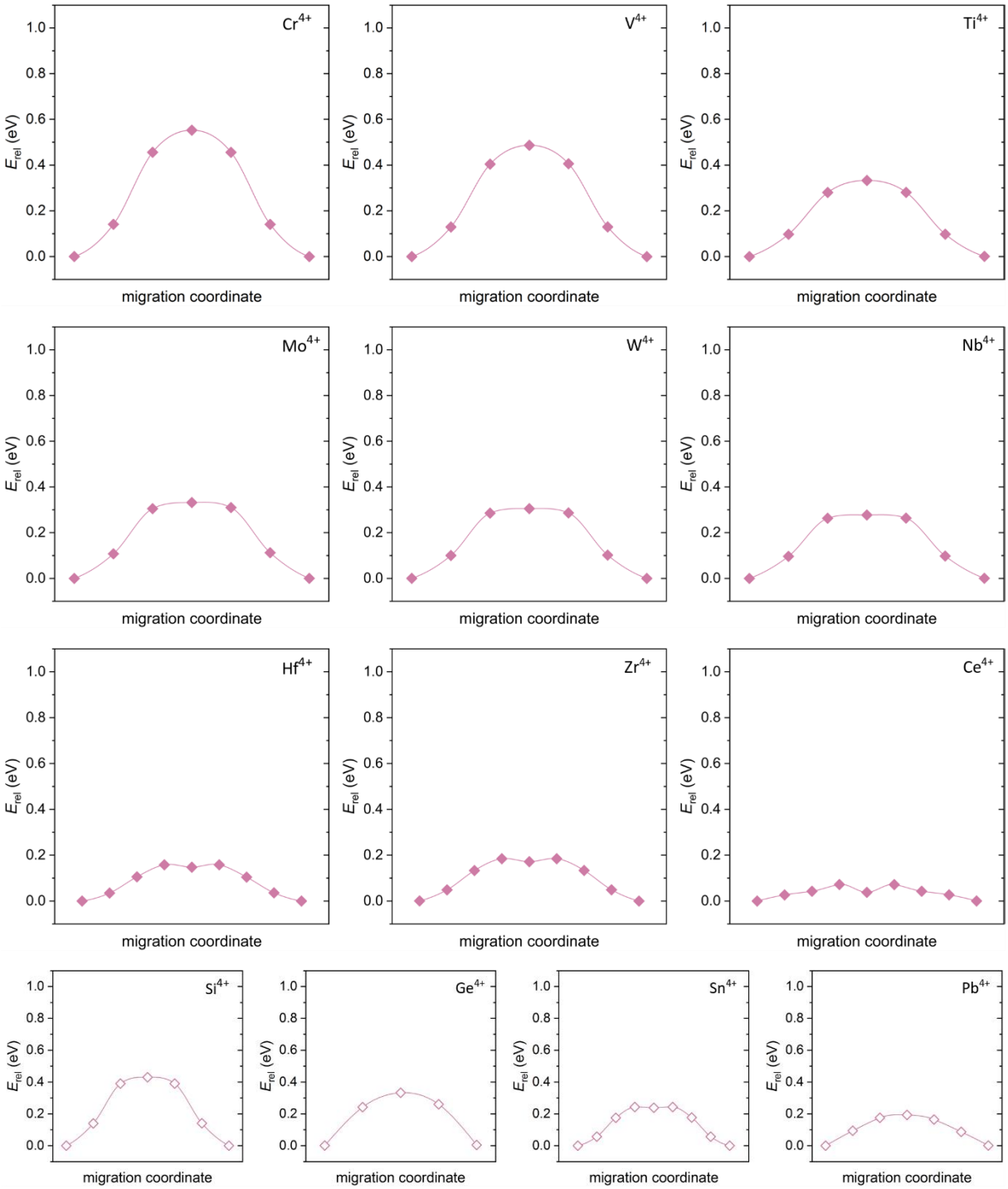

Figure S20. Energy profiles of interstitialcy-like migration in 180° in Na*M*P containing different M^{4+} cations.

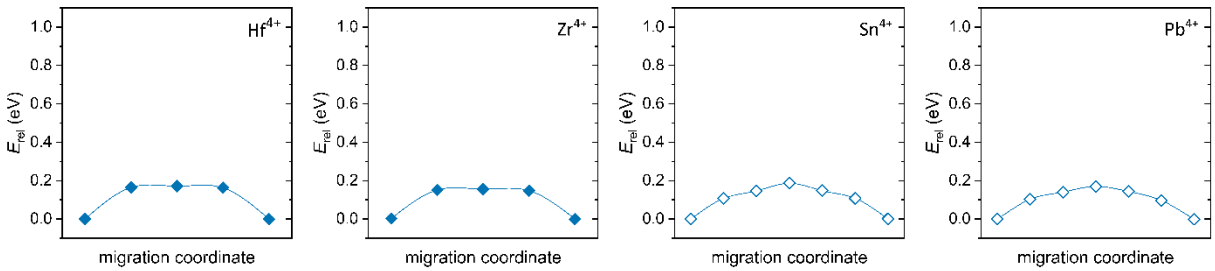

Figure S21. Energy profiles of interstitialcy-like migration in 90° in Na*M*Si containing different M^{4+} cations.

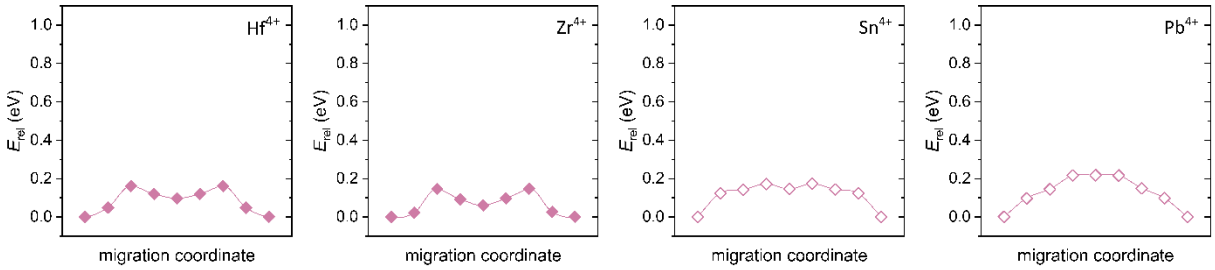

Figure S22. Energy profiles of interstitialcy-like migration in 180° in Na*M*Si containing different M^{4+} cations.

3.3 Migration Energy

The migration energy E_{mig} for both Na*M*P and Na*M*Si and configuration energy E_{conf} of the transient state corresponding to configuration (0b) or (0c) and configuration (3b) or (3c) involved in the migration are compared. Figure S23 (a) depicts E_{mig} as a function of E_{conf} for Na*M*P, revealing a linear correlation. This suggests that E_{mig} is primarily governed by the stability of the metastable transient state corresponding to configuration (0b) and (0c). Nevertheless, this correlation is not observed for Na*M*Si, as shown by the plot of E_{mig} versus E_{conf} for Na*M*Si in Figure S23 (b).

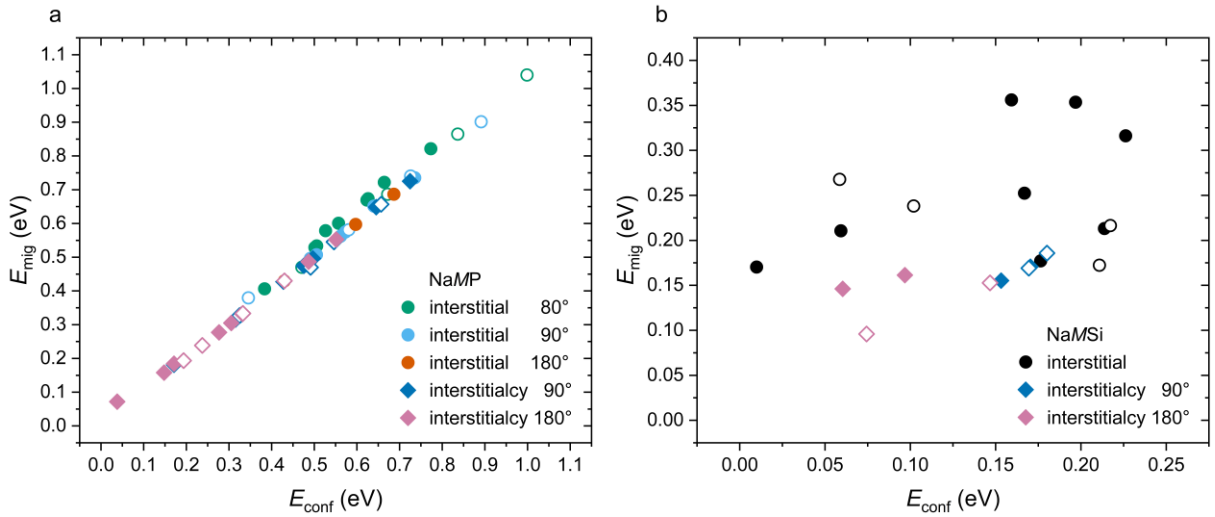

Figure S23. Migration energy E_{mig} of interstitial- and interstitialcy-like migration in 80°, 90°, 180° direction for (a) Na*M*P and (b) Na*M*Si as a function of configuration energy E_{conf} of the metastable transient state corresponding to configuration (0b) or (3b) and configuration (0c) or (3c) involved in the interstitial- and interstitialcy-like migration, respectively.

3.4 Bottleneck of Interstitial-like Migration

During the Na^+ ion migration, the ions jump from Na1 sites to Na2 sites or vice versa according to the interstitial or interstitialcy mechanism. The Na^+ ions pass through bottlenecks formed by the O^{2-} ions of the PO_4/SiO_4- and MO_6-polyhedra, as shown in Figure S 24 for the interstitial migration.

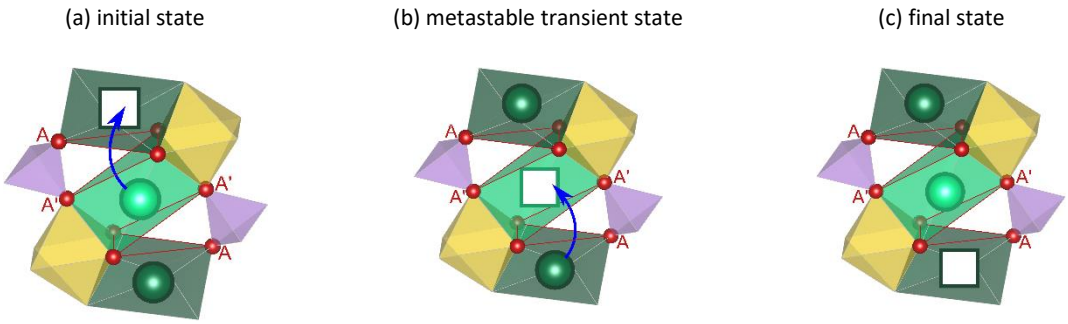

Figure S 24. (a) Initial, (b) metastable transient, and (c) final state of the interstitial-like mechanism, shown with blue arrows. (a) The Na1 ion jumps onto an adjacent vacant Na2 site; (b) The metastable transition state with one V_{Na1} and two occupied Na2 sites is formed. Subsequently, the Na2 ion jumps onto the V_{Na1}; (c) In the final state, the Na1 and one Na2 sites are occupied. The bottlenecks A and A' of the migration pathway formed by PO_4/SiO_4- and MO_6-polyhedra edges are depicted as red triangles. Key: Na^+ vacancy (empty box), Na1 (light green), Na2 (dark green), MO_6 (yellow), PO_4/SiO_4 (purple), O (red).

The impact of the size of these bottlenecks on the migration energy is investigated using the example of the interstitial migration. In the interstitial migration, the bottlenecks denoted as A are located near the Na2 sites, while the bottlenecks denoted as A' are located near the Na1 site.

The area *A* of the bottlenecks A and A' as a function of the size of the M^{4+} cations as well as the migration energy E_{mig} as a function of the bottleneck areas for the interstitial migration in Na*M*Si are shown in Figure S25. The bottlenecks in the initial/final state of the migration are investigated. The size of the bottlenecks increase approximately linearly with the size of the M^{4+} cations as the NaSICON skeleton expands. The enlargement of the bottleneck consequently leads to a decrease in E_{mig}.

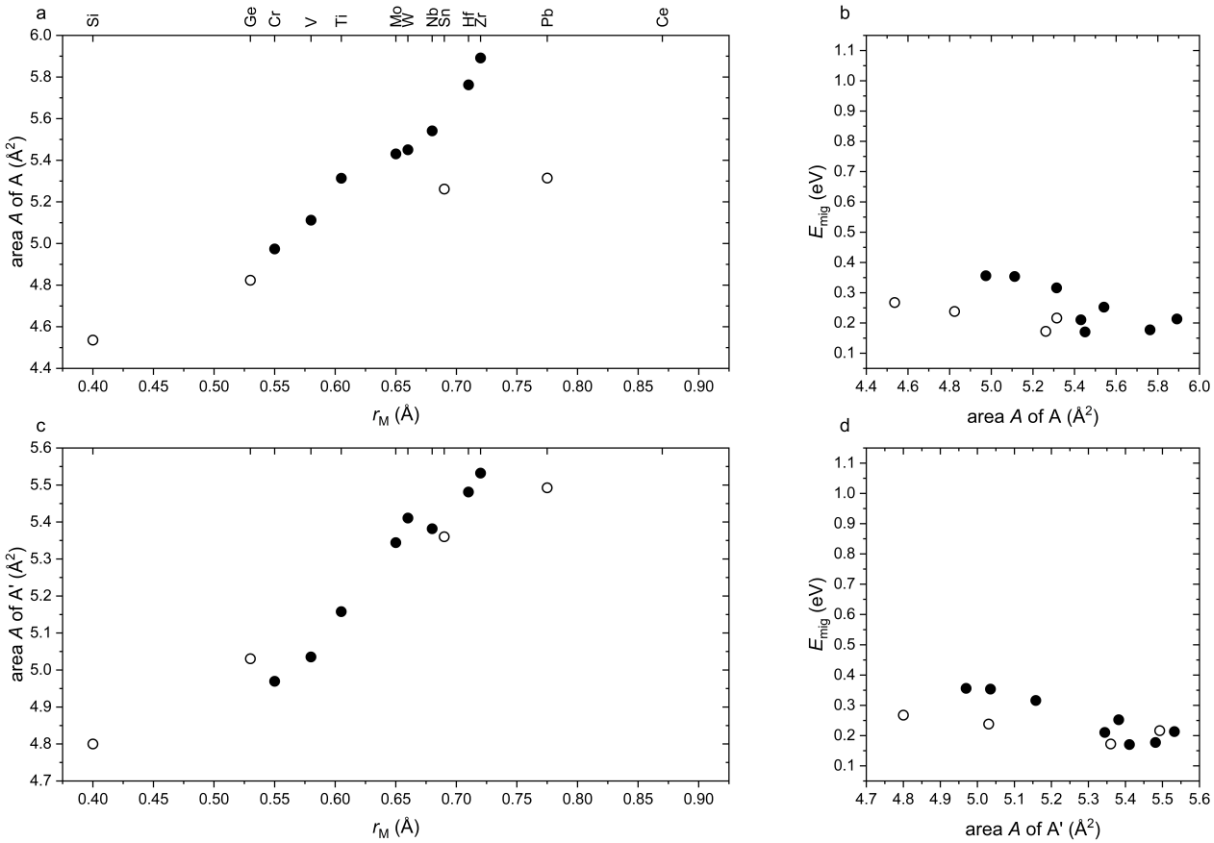

Figure S25. Area *A* of the bottleneck (a) A and (c) A' as a function of the Shannon radii r_M[1] of the M^{4+} cations, and migration energy E_{mig} as a function of the area of the bottleneck (b) A and (d) A' for the Na^+ interstitial-like migration in Na*M*Si with different M^{4+} cations (filled symbols: M^{4+} transition metals, empty symbols: M^{4+} main group cations). The areas of the bottlenecks in the initial/final state are shown.

References

1 R. D. Shannon, Revised effective ionic radii and systematic studies of interatomic distances in halides and chalcogenides, *Acta Crystallogr. A*, 1976, **32**, 751–767.